Lett., **1987**, *79* (1-2), 195-200.

[67] Combs, C.K.; Karlo, J.C.; Kao, S.C.; Landreth, G.E. beta-Amyloid stimulation of microglia and monocytes results in TNFalpha-dependent expression of inducible nitric oxide synthase and neuronal apoptosis. *J. Neurosci.*, **2001**, *21* (4), 1179-1188.

[68] Hashioka, S.; Monji, A.; Ueda, T.; Kanba, S.; Nakanishi, H. Amyloid-beta fibril formation is not necessarily required for microglial activation by the peptides. *Neurochem. Int.*, **2005**, *47* (5), 369-376.

[69] Hashioka, S.; Han, Y.H.; Fujii, S.; Kato, T.; Monji, A.; Utsumi, H.; Sawada, M.; Nakanishi, H.; Kanba, S. Phosphatidylserine and phosphatidylcholine-containing liposomes inhibit amyloid beta and interferon-gamma-induced microglial activation. *Free Radic. Biol. Med.*, **2007**, *42* (7), 945-954.

[70] Meda, L.; Cassatella, M.A.; Szendrei, G.I.; Otvos Jr. L.; Baron, P.; Villalba, M.; Ferrari, D.; Rossi, F. Activation of microglial cells by beta-amyloid protein and interferon-gamma. *Nature*, **1995**, *374* (6523), 647-650.

[71] McGeer, P.L.; McGeer, E.G. NSAIDs and Alzheimer disease: epidemiological, animal model and clinical studies. *Neurobiol. Aging*, **2007**, *28* (5), 639-647.

[72] Nelson, R.L.; Guo, Z.; Halagappa, V.M.; Pearson, M.; Gray, A.J.; Matsuoka, Y.; Brown, M.; Martin, B.; Iyun, T.; Maudsley, S.; Clark, R.F.; Mattson, M.P. Prophylactic treatment with paroxetine ameliorates behavioral deficits and retards the development of amyloid and tau pathologies in 3xTgAD mice. *Exp. Neurol.*, **2007**, *205* (1), 166-176.

[73] Mowla, A.; Mosavinasab, M.; Pani, A. Does fluoxetine have any effect on the cognition of patients with mild cognitive impairment? A double-blind, placebo-controlled, clinical trial. *J. Clin. Psychopharmacol.*, **2007**, *27* (1), 67-70.

[74] Duman, R.S. Depression: a case of neuronal life and death? *Biol. Psychiatry*, **2004**, *56* (3), 140-145.

[75] Malberg, J.E.; Eisch, A.J.; Nestler, E.J.; Duman, R.S. Chronic antidepressant treatment increases neurogenesis in adult rat hippocampus. *J. Neurosci.*, **2000**, *20* (24), 9104-9110.

[76] Vermetten, E.; Vythilingam, M.; Southwick, S.M.; Charney, D.S.; Bremner, J.D. Long-term treatment with paroxetine increases verbal declarative memory and hippocampal volume in posttraumatic stress disorder. *Biol. Psychiatry*, **2003**, *54* (7), 693-702.

[77] Ekdahl, C.T.; Classen, J.H.; Bonde, S.; Kokaia, Z.; Lindvall; O. Inflammation is detrimental for neurogenesis in adult brain. *Proc. Natl. Acad. Sci. USA*, **2003**, *100* (23), 13632-13637.

Received: July 24, 2008 **Revised: September 24, 2008** **Accepted: September 30, 2008**

Psychiatry and Clinical Neurosciences 2009; 63: 423–425 doi:10.1111/j.1440-1819.2009.01952.x

Short Communication

Attenuated prefrontal activation during a verbal fluency task in remitted major depression

Go Okada, MD, PhD,[1]* Yasumasa Okamoto, MD, PhD,[1] Hidehisa Yamashita, MD, PhD,[1] Kazutaka Ueda, PhD,[2] Hiroshi Takami, MD, PhD[3] and Shigeto Yamawaki, MD, PhD[1]

[1]*Department of Psychiatry and Neurosciences, Division of Frontier Medical Science, Programs for Biomedical Research, Graduate School of Biomedical Sciences, Hiroshima University, Hiroshima,* [2]*Research Center for Advanced Science and Technology, University of Tokyo, Tokyo and* [3]*Kamo Psychiatry Medical Center, Hiroshima, Japan*

The aim of the present study was to investigate whether a functional abnormality in the left prefrontal cortex observed in patients with major depression performing a verbal fluency task is present after remission of depression. Functional magnetic resonance imaging was used to study changes in cerebral blood oxygenation in eight remitted patients with major depression and 10 healthy control subjects during a verbal fluency task. Compared to the control subjects, the patients had a reduced response in the left prefrontal cortex (middle frontal gyrus, Brodmann area 10). These findings suggest the presence of dysfunction in the left prefrontal cortex during remission in major depression.

Key words: anterior cingulate cortex, depression, magnetic resonance imaging, prefrontal cortex, remission.

IMPAIRED COGNITIVE FUNCTION is a common and disabling feature of depression, both during an acute depressive episode and in the remitted state. A number of studies in recent years have used functional magnetic resonance imaging (fMRI) to study brain activation associated with cognitive activity in patients with depression. Although these studies have provided conflicting results due to the fact that most studies have used different cognitive tasks,[1–6] we reported previously that depressed patients showed significantly attenuated activations in the left prefrontal cortex (PFC) during a verbal fluency task, when compared to control subjects.[7] In the present study we used the same activation paradigm to investigate changes in brain activation in remitted patients with major depression.

METHODS

The study participants were eight remitted patients with major depression (six men, two women, aged 35–55 years) and 10 healthy volunteers (eight men, two women, aged 34–57 years) with no history of neurological or psychiatric illness. All subjects were right-handed according to the Edinburgh Handedness Inventory. All of the patients were inpatients at Hiroshima University Medical Hospital, diagnosed by three experienced clinicians as having major depressive disorder, but no other major disorders according to DSM-IV criteria.[8] Remission was defined as ≤7 on the 17-item Hamilton Rating Scale for Depression (HRSD).[9] Their mean score on the HRSD was 5.3 ± 1.4. The duration of the remitted phase in the patients prior to the study was 8.4 ± 3.3 days. All were medicated as follows: four patients were taking 200 mg fluvoxamine, and the other four were taking either 50 mg fluvoxamine, 150 mg clomipramine, 225 mg amoxapine, or 20 mg paroxetine. Seven of

Correspondence: Go Okada, MD, PhD, Department of Psychiatry and Neurosciences, Division of Frontier Medical Science, Programs for Biomedical Research, Graduate School of Biomedical Sciences, Hiroshima University, 1-2-3 Kasumi, Minami-ku, Hiroshima 734-8551, Japan. Email: goookada@hiroshima-u.ac.jp
Received 16 July 2008; revised 15 January 2009; accepted 27 January 2009.

the patients and all of the healthy volunteers participated in the previous study.[7] The examinations were conducted under a protocol approved by the Ethics Committee of Hiroshima University School of Medicine. After complete description of the study to the subjects, written informed consent was obtained.

The verbal fluency activation paradigm, echo planar imaging acquisition, image processing, measurements of verbal fluency test performance, and data analysis were performed according to methods described previously.[7]

RESULTS

No significant differences were detected between the patients and the control subjects for verbal fluency performance (patients: mean, 21.8 ± 3.7 words; control subjects: mean, 25.8 ± 8.3 words; $P = 0.220$).

For both groups, verbal fluency task resulted in the significant activation of the left PFC ($P < 0.001$ uncorrected on the single voxel level and $P < 0.05$ corrected on the cluster level; Fig. 1a,b). The control group also had significant activation in the cingulate cortex and thalamus, while the depressed group did not ($P < 0.001$ uncorrected on the single voxel level and $P < 0.05$ corrected on the cluster level; Fig. 1a,b). A direct comparison on two-sample *t*-test at each voxel of the brain activation in the two groups showed that the control group had significantly greater activations than the patients in a small portion of the left PFC (middle frontal gyrus, Brodmann area 10; $P < 0.001$ uncorrected on the single voxel level, extent threshold of 10 voxels; Fig. 1c).

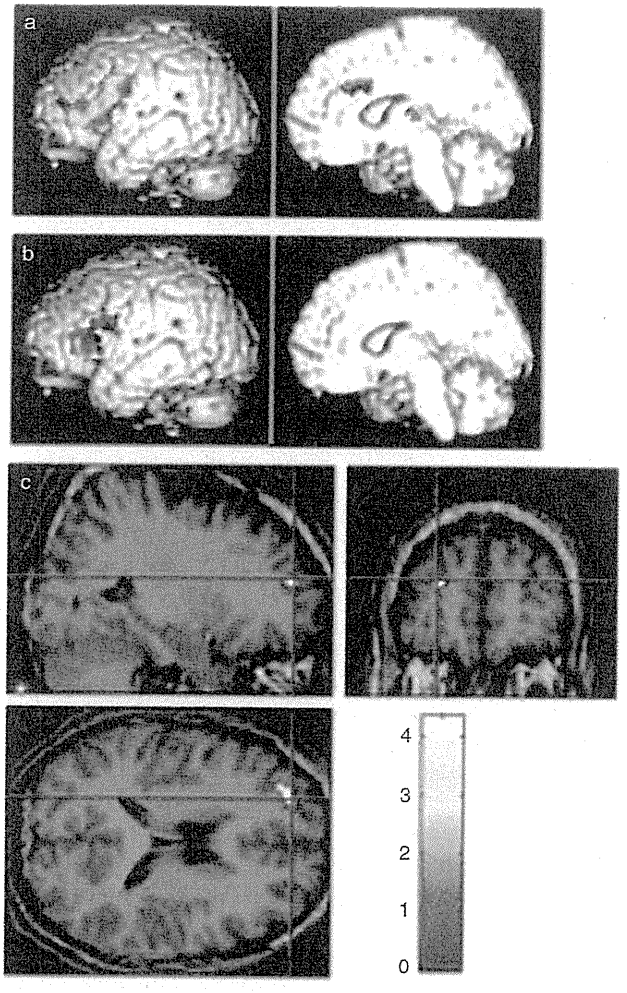

Figure 1. (a) Statistical parametric maps of brain regions (second-level analysis for 10 control subjects) showing significant activation associated with the verbal fluency task. (b) Statistical parametric maps of brain regions (second-level analysis for eight remitted patients with major depression) showing significant activation associated with the verbal fluency task. (c) Statistical parametric maps of brain regions in which 10 controls had significantly greater activation in a verbal fluency task than eight remitted patients with major depression. T-levels of activation are color-coded from red to yellow.

DISCUSSION

Within this verbal fluency neural network, brain activation in the left PFC remained impaired in patients in remission during the short observation period in spite of their clear clinical improvement. In our previous study there was no significant difference in this area of activation between depressive patients in recovery (defined as maintaining a score of ≤7 on the 17-item HRSD for >3 months) and healthy volunteers.[10] This result suggests that the brain activity may take longer to return to a normal level than the observed mood improvement.

Results of recent studies suggest that functional neuroimaging is a more sensitive assay of cognitive processing than behavioral measures.[11] Therefore, the neurophysiological problems identified in the present study may reflect subtle cognitive deficits of remitted patients. The present findings, however, are limited by the relatively small group size and potential medication effects. A second limitation is the short period of the remitted phase in the present patients. Although they were asymptomatic at examination, they fulfilled criteria for partial remission on

DSM-IV-TR. Further longitudinal studies using larger numbers of unmedicated subjects are required to elucidate the neurophysiological abnormalities in major depression.

ACKNOWLEDGMENTS

This study was partly supported by KAKENHI (20790841).

REFERENCES

1 Barch DM, Sheline YI, Csernansky JG, Snyder AZ. Working memory and prefrontal cortex dysfunction: Specificity to schizophrenia compared with major depression. *Biol. Psychiatry* 2003; **53**: 376–384.
2 Hugdahl K, Rund BR, Lund A *et al.* Brain activation measured with fMRI during a mental arithmetic task in schizophrenia and major depression. *Am. J. Psychiatry* 2004; **161**: 286–293.
3 Fahim C, Stip E, Mancini-Marie A *et al.* Abnormal prefrontal and anterior cingulate activation in major depressive disorder during episodic memory encoding of sad stimuli. *Brain Cogn.* 2004; **54**: 161–163.
4 Harvey PO, Fossati P, Pochon JB *et al.* Cognitive control and brain resources in major depression: An fMRI study using the n-back task. *Neuroimage* 2005; **26**: 860–869.
5 Rose EJ, Simonotto E, Ebmeier KP. Limbic over-activity in depression during preserved performance on the n-back task. *Neuroimage* 2006; **29**: 203–215.
6 Fitzgerald PB, Srithiran A, Benitez J *et al.* An fMRI study of prefrontal brain activation during multiple tasks in patients with major depressive disorder. *Hum. Brain Mapp.* 2008; **29**: 490–501.
7 Okada G, Okamoto Y, Morinobu S, Yamawaki S, Yokota N. Attenuated left prefrontal activation during a verbal fluency task in patients with depression. *Neuropsychobiology* 2003; **47**: 21–26.
8 American Psychiatric Association. *Diagnostic and Statistical Manual of Mental Disorders*, 4th edn. American Psychiatric Association, Washington, DC, 1994.
9 Frank E, Prien RF, Jarrett RB *et al.* Conceptualization and rationale for consensus definitions of terms in major depressive disorder. Remission, recovery, relapse, and recurrence. *Arch. Gen. Psychiatry* 1991; **48**: 851–855.
10 Takami H, Okamoto Y, Yamashita H, Okada G, Yamawaki S. Attenuated anterior cingulate activation during a verbal fluency task in elderly patients with a history of multiple-episode depression. *Am. J. Geriatr. Psychiatry* 2007; **15**: 594–603.
11 Goldberg TE, Weinberger DR. Genes and the parsing of cognitive processes. *Trends. Cogn. Sci.* 2004; **8**: 325–335.

ORIGINAL RESEARCH

A.M. Tokumaru
Y. Saito
S. Murayama
K. Kazutomi
Y. Sakiyama
M. Toyoda
M. Yamakawa
H. Terada

Imaging-Pathologic Correlation in Corticobasal Degeneration

BACKGROUND AND PURPOSE: The clinical diagnosis of corticobasal degeneration (CBD) is often difficult due to varied clinical manifestations. In 4 patients with neuropathologically confirmed CBD, characteristic imaging findings and correlations with neuropathologic features were evaluated. Furthermore, imaging findings in CBD were compared with neuropathologically confirmed progressive supranuclear palsy (PSP) for a differential diagnosis.

MATERIALS AND METHODS: Four patients with neuropathologically confirmed CBD were studied. We evaluated the area of the tegmentum in the midsagittal plane, subcortical white matter (SCWM) abnormality, asymmetric cerebral atrophy, and signal-intensity abnormality in the subthalamic nuclei on MR imaging and compared them with histopathologic findings. Then, MR imaging findings in CBD were compared with those in 13 patients with PSP.

RESULTS: On MR imaging, 3 patients had asymmetric cerebral atrophy extending to the central sulcus. On midsagittal sections, the mean midbrain tegmentum area was 66 mm^2, being markedly smaller than normal, but there was no significant difference between PSP and CBD. All patients had signal-intensity abnormalities of the SCWM, constituting primary degeneration neuropathologically; however, no diffuse signal-intensity abnormality in the SCWM existed in the 13 patients with PSP. In 3 patients, T1-weighted images showed symmetric high signal intensity in the subthalamic nuclei. Neuropathologically, these areas showed characteristic CBD. MR imaging signal-intensity changes also existed in 4 patients with PSP; however, subthalamic nucleus degeneration was more severe in PSP than in CBD.

CONCLUSIONS: In cases with midbrain tegmentum atrophy and signal-intensity changes in the subthalamic nuclei, the differential diagnosis distinguishing CBD from PSP based on MR imaging alone was difficult. White matter lesions and asymmetric atrophy can be useful for a differential diagnosis.

Corticobasal degeneration (CBD) is a slowly progressive disorder with a clinically asymmetric onset characterized by apraxia, dystonia, postural instability, and an akinetic-rigid syndrome that does not respond to levodopa. However, clinical phenotypes of Alzheimer disease, Pick disease, and progressive supranuclear palsy (PSP) with similar characteristic features often make a differential diagnosis distinguishing these entities from CBD difficult in clinical practice.

Koyama et al[1] recently reported asymmetric cerebral atrophy with dominance contralateral to the more clinically affected side, hyperintensity in the subcortical white matter (SCWM) in the frontotemporal area on fluid-attenuated inversion recovery (FLAIR), and atrophy of the midbrain tegmentum as new imaging findings of clinically diagnosed CBD, but no imaging findings in pathologically proved cases have been reported.[3,4] We encountered 4 patients with neuropathologically confirmed CBD in whom the findings could be compared with those of MR imaging. Cortical symptoms were unclear in 3, and it was difficult to make a diagnosis on the basis of clinical symptoms alone because of underlying dementia. Although the number of cases was small, because the neuropathology and images were collated in all cases, this study was significant with regard to the objectivity of the imaging findings associated with an accurate diagnosis. We also thought that it was important to identify differences in imaging findings between CBD and PSP, in which severe atrophy of the midbrain tegmentum has been reported.[1,2] Therefore, MR imaging findings in CBD were compared with those in 13 cases of neuropathologically confirmed PSP.

Received January 3, 2009; accepted after revision May 12.

From the Departments of Diagnostic Radiology (A.M.T., M.T., M.Y.), Neuropathology (S.M.), and Neurology (K.K.), Tokyo Metropolitan Medical Center of Gerontology, Itabashi-Ku, Tokyo, Japan; Department of Neuropathology (Y. Saito), National Center of Neurology and Psychiatry, Kodaira, Tokyo, Japan; Department of Neurology (Y. Sakiyama), Jichi Medical College, Omiya, Saitama, Japan; and Department of Radiology (H.T.), Toho University, Sakura Medical Center, Sakura, Chiba, Japan.

Please address correspondence to Aya M. Tokumaru, MD, PhD, Department of Radiology, Tokyo Metropolitan Medical Center of Gerontology, 35-2 Sakaecho, Itabashi-ku, Tokyo 173-0015, Japan; e-mail: tokumaru@tmghig.jp

DOI 10.3174/ajnr.A1721

Materials and Methods

Patients

Four patients (1 man, 3 women) with neuropathologically confirmed CBD were evaluated retrospectively. The patients' mean age at death was 70.8 years (range, 67–74 years). Table 1 lists the patient characteristics. The MR imaging findings in the patients with CBD (Table 2) were compared with those in 13 patients with neuropathologically confirmed PSP. All 13 patients with PSP were men, with a mean age at death of 78.3 years (range, 64–87 years). For the comparative evaluation of atrophy of the midbrain tegmentum, 10 aged-matched control subjects (4 men and 6 women) with no neuropathologic degenerative disease or cerebrovascular disorder were selected (mean age at death, 74.6 years; range, 68–83 years).

MR Imaging Examinations

All studies were performed with a 1.5T MR imaging unit (Signa Excite HD; GE Healthcare, Milwaukee, Wis). Axial T2-weighted images (TR/TE, 4300/89 ms; NEX, 2; FOV, 220 mm; section thickness, 5 mm with a section gap of 1 mm) and FLAIR images (TR/TE, 10,002/106 ms; TI, 2500 ms; NEX, 1; section thickness, 5 mm with a gap of 1 mm), sagittal T1-weighted images (TR/TE, 600/14 ms; NEX, 2; section thickness, 5 mm with a gap of 1 mm), or sagittal spoiled gradient-echo

Table 1: Clinical findings of pathologically confirmed corticobasal degeneration

Case No.	Age at Onset (yr)	Sex	Duration (yr)	Rigidity	Dystonia	Pyramidal Signs	Cortical Dysfunction	Vertical Gaze Palsy	Dementia	CDx
1	74	F	10	Lt>Rt	–	–	Ocular apraxia	+	Mute	PSP?
2	68	F	6	Lt>Rt			Apraxia (Lt hand)	±	+ Severe akinetic mute	AD
3	67	M	3	Rt>Lt			No cortical sign	+	+ Severe	PDD
4	74	F	6	Rt>Lt	–	–	–	+	+ Severe	CBD

Note:—CBD indicates corticobasal degeneration; PSP?, progressive supranuclear palsy suspected; CDx, clinical diagnosis; AD, Alzheimer disease; PDD, Parkinson disease with dementia; –, no symptom; +, obvious symptom; ±, suspicious symptom; Lt, left; Rt, right.

Table 2: MR imaging findings of neuropathologically confirmed corticobasal degeneration

Case No.	Atrophy (Dominant Cerebral Hemisphere)	White Matter Hyperintensity on FLAIR		Hyperintensity on T1WI in Bil Subthalamic Nucleus
		Precentral Gyrus	Frontal Lobe	
1	Rt frontal operculum and convexity	–	+	+
2	Bil frontal convexity	–	+	+
3	Lt frontoparietal	Bil	+	+
4	Rt frontoparietal	Rt	+	+

Note:—FLAIR indicates fluid-attenuated inversion recovery; T1WI = T1-weighted imaging; Bil, bilateral; –, no signal abnormality; +, obvious signal abnormality.

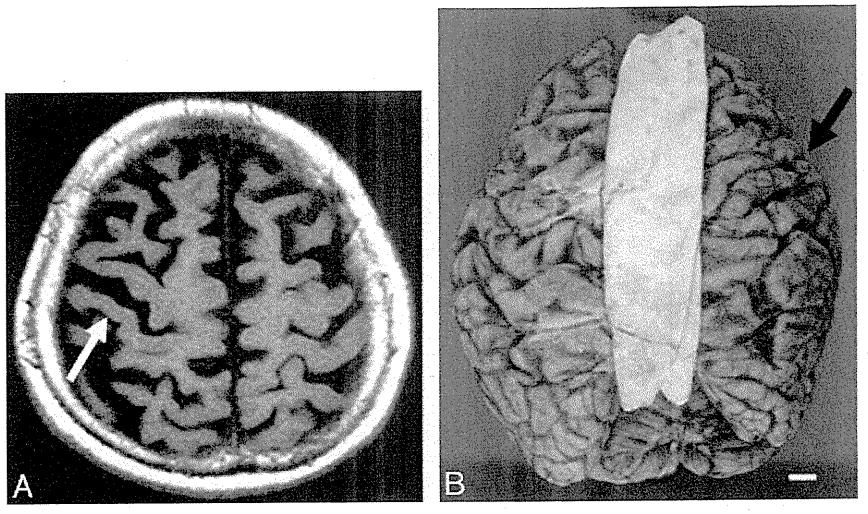

Fig 1. Corticobasal degeneration, case 1. An 84-year-old woman. *A*, Axial T2-weighted image shows right-side-dominant atrophy including the central sulcus (*arrow*). *B*, A macrospecimen of this patient shows right-frontal-dominant atrophy (*arrow*).

images (TR/TE, 21/6 ms; TI, 0 ms; flip angle, 20°) were obtained in all patients with CBD and PSP and healthy controls. Spin-echo coronal T1-weighted images (TR/TE, 600/14 ms; NEX, 2; section thickness, 5 mm with a gap of 1 mm) were obtained in 3 of the 4 patients with CBD, 7 of the 13 patients with PSP, and the 10 age-matched healthy controls. In 1 patient with CBD and 3 with PSP, T1-weighted coronal spin-echo images could not be obtained; spoiled gradient-echo imaging (TR/TE, 21/6 ms; TI, 0 ms; flip angle, 20°) was selected instead. These patients and 3 other patients with PSP without coronal sections were excluded from evaluation of the T1-weighted signal intensity. The area of the midbrain tegmentum was measured on an MR imaging workstation by using the method of Oba et al[2] in a T1-weighted midsagittal section through the center of the interpeduncular cistern and the center of the cerebral aqueduct. Two neuroradiologists (A.M.T. and M.T.) performed these measurements blindly, twice at different times.

The localization and laterality of cerebral atrophy, signal intensity in the subthalamic nuclei, and signals in the SCWM were only qualitatively investigated because of the limitations of the retrospective nature of pathologically confirmed cases. The 2 neuroradiologists blindly investigated images of 4 patients with CBD, 13 patients with PSP, and 10 healthy controls twice at different times and visually evaluated the following points: 1) the presence or absence and laterality of cerebral atrophy and whether the atrophy included the central sulcus on T1-weighted imaging, 2) the presence or absence and localization of a high signal intensity in the SCWM on T2-weighted or FLAIR imaging, and 3) the presence or absence of an increase in the signal intensity in the subthalamic nuclei in the coronary view on T1-weighted imaging.

Neuropathologic Examinations

Informed consent for autopsy was obtained from all of the patients or their families. All serial autopsy cases were examined with the Brain Bank Aging Research protocol, irrespective of clinical diagnosis.[3] At autopsy, after taking photographs of the whole brain, we serially sectioned the nondominant hemisphere or the hemisphere spared from focal lesions at a 7-mm thickness. The cerebrum was cut on the coronal plane; the brain stem, on the axial plane; and the cerebellum, on

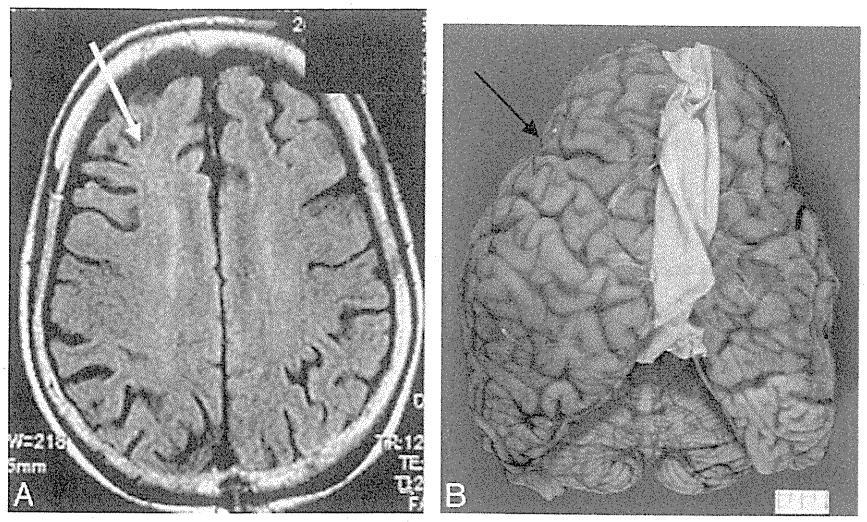

Fig 2. Corticobasal degeneration, case 2. A 74-year-old woman. *A*, An axial fluid-attenuated inversion recovery image 3 years before autopsy shows no obvious asymmetric atrophy. Subcortical hyperintensity is shown in the right frontal white matter (*white arrow*). *B*, A macrospecimen of this patient shows mild frontal atrophy with some asymmetry (*arrow*).

the sagittal plane. Photographs were taken of all sections. Small pieces of the anterior amygdala; posterior hippocampus; frontal, temporal, and occipital poles; supramarginal gyrus; and rostral midbrain were directly fixed in 4% paraformaldehyde for 48 hours and prepared for immunohistochemical and ultrastructural studies. The remaining sections were quick frozen and stored at −80°C. The hemisphere kept for morphologic examinations was fixed in 20% neutral buffered formalin for 7–13 days and cut into 7-mm-thick sections, similar to those in the contralateral hemisphere. Paraffin-embedded sections of representative areas of the brain were examined.

The selected anatomic structures included those recommended by the Consortium to Establish a Registry for Alzheimer Disease,[4] the Consensus Guidelines for the Diagnosis of Dementia with Lewy Bodies,[5,6] Braak and Braak's recommendation,[7] and the Diagnostic Criteria of Corticobasal Degeneration and Progressive Supranuclear Palsy.[8,9] These included the frontal pole; temporal pole; cingulate gyrus; second frontal gyrus; accumbens and septal nuclei; amygdala; basal nucleus of Meynert; second temporal gyrus; anterior hippocampus with entorhinal and transentorhinal cortices; basal ganglia and hypothalamus with mamillary bodies; subthalamic nucleus; posterior hippocampus; thalamus with the red nucleus; motor cortex; parietal lobe with the intraparietal sulcus; visual cortex; midbrain; upper and middle pons; medulla oblongata; cerebellar vermis; dentate nucleus; and multiple cervical, thoracic, and lumbar levels of the spinal cord.

Six-micrometer-thick sections were routinely stained with hematoxylin-eosin and the Klüver-Barrera method. Selected sections were stained with the modified methenamine, Gallyas-Braak, and Bielschowsky silver staining for age-related changes, with Congo red for amyloid β deposition and elastica-Masson trichrome staining for vascular changes.

Immunohistochemistry

Six-micrometer-thick serial sections were immunohistochemically stained by using a 20NX autostainer (Ventana, Tucson, Ariz), as previously described. The antibodies applied to all the cases were the following: antiphosphorylated α-synuclein (psyn); phosphorylated tau (ptau) (AT8, monoclonal; Innogenetic, Temse, Belgium); 3-repeat tau (RD3, amino acids 209–224, monoclonal, Upstate; Millipore, Lake Placid, NY); 4-repeat tau (RD4, amino acid 275–291, monoclonal, Upstate; Millipore); amyloid β 11–28 (12B2, monoclonal; IBL, Maebashi, Japan); glial fibrillary acidic protein (polyclonal; DAKO, Glostrup, Denmark); HLA-DR (monoclonal, CD68; DAKO); phosphorylated neurofilament (monoclonal SMI31; Sternberger Immunochemical, Baltimore, Md); myelin basic proteins (polyclonal, DAKO); and ubiquitin (polyclonal, DAKO) antibodies.

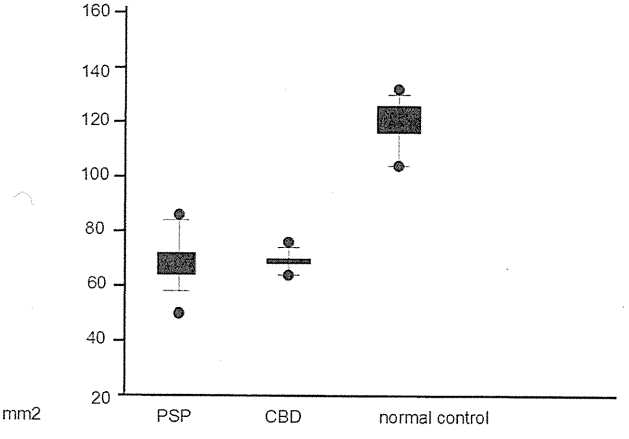

Fig 3. Scatterplot (mean, SD, and range) of the area of the midbrain in patients with progressive supranuclear palsy (PSP), corticobasal degeneration (CBD), and age-matched healthy controls. There was no individual overlap of the midbrain tegmental area between the healthy controls and patients with CBD and PSP, apparently showing that severe atrophy of the midbrain tegmentum was present in patients with CBD and PSP.

In addition to the routine neuropathologic examination mentioned above, studies were performed at sites of MR imaging signal-intensity abnormalities or atrophy to correlate the radiologic and pathologic findings. To compare them with MR imaging findings, 2 neuropathologists investigated the following points in addition to routine examinations: 1) the macroscopic presence or absence, laterality, and localization of cerebral atrophy at the time of sectioning the brain and after fixation, 2) the macroscopic presence or absence of atrophy of the midbrain tegmentum at the time of sectioning the brain and after fixation, 3) the presence or absence and degree of degeneration of the subthalamic nuclei, and 4) the presence or absence of a lesion in the SCWM and whether the lesion constituted primary or secondary degeneration in CBD. For brain samples, 7-mm coronal sections of the lateral region passing the mamillary body vertical to the hippocampal structure were prepared. Abnormal intensi-

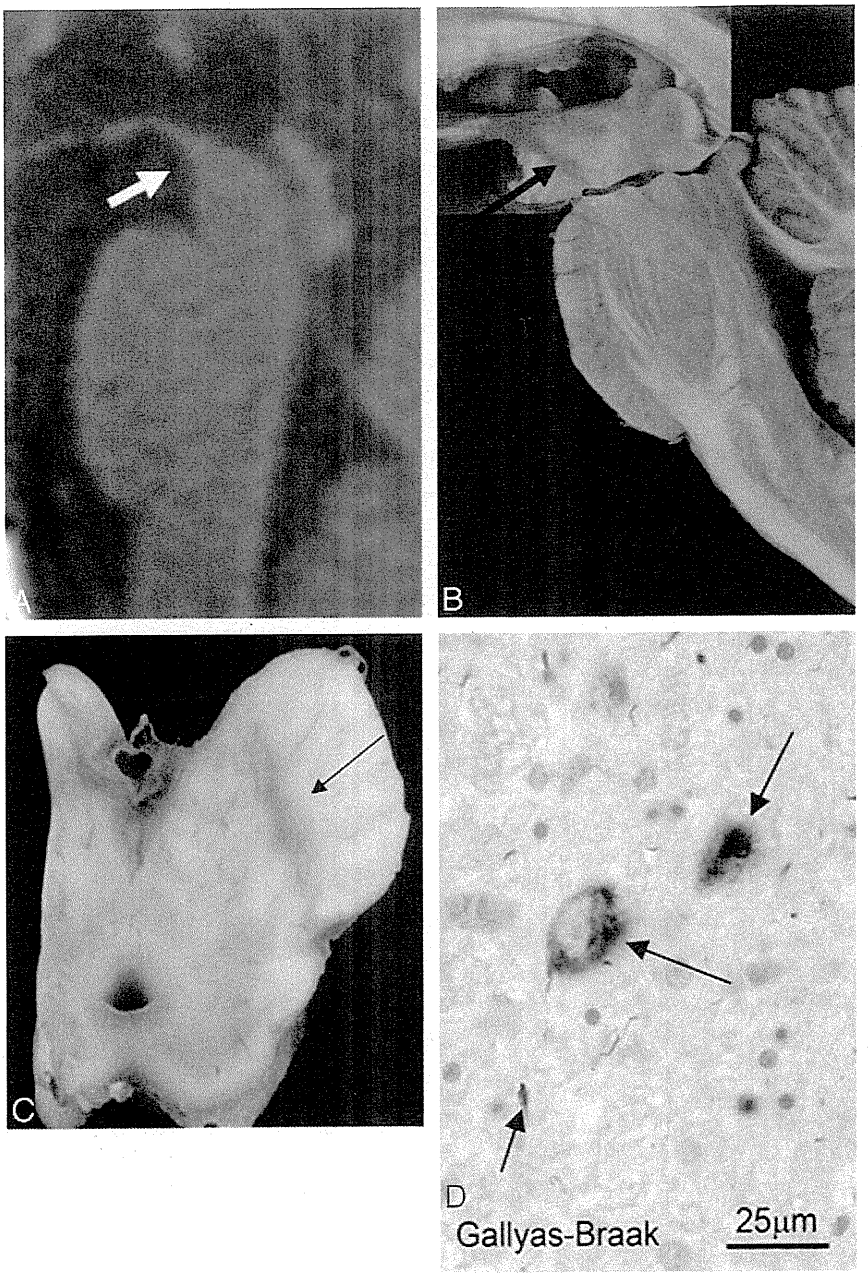

Fig 4. Corticobasal degeneration (CBD), case 1. An 84-year-old woman. *A*, T1-weighted midsagittal image clearly shows atrophy of the midbrain tegmentum (*arrow*). The area of the midbrain tegmentum is 73 mm^2. *B*, A macroscopic specimen of the midbrain shows marked atrophy (*arrow*). *C*, A macroscopic view of the midbrain shows discoloration of the substantia nigra (*arrow*). *D*, A microscopic view of the substantia nigra (Gallyas-Braak stain) shows argyrophilic threads and granular or fibrous inclusion bodies (*arrows*). These are consistent with CBD.

ties on MR imaging were collated with the pathologic preparations as accurately as possible, with the line passing the mamillary body vertical to the hippocampal structure as the baseline, and new pathologic sections were cut out as needed.

Results

Asymmetric Cerebral Atrophy

Asymmetric cerebral atrophy was observed in 3 of 4 patients with predominance contralateral to the more clinically affected side. In all 3 patients, cerebral atrophy affected the area including the central sulcus. In 1 patient, the radiologic and pathologic findings of predominantly frontal lobe atrophy were correlated (case 1, Fig 1*A*, -*B*). In 1 patient (case 2, Fig 2*A*, -*B*) in whom the interval between MR imaging and autopsy was 3 years, asymmetric cortical atrophy was difficult to detect on MR imaging, but frontal atrophy with some asymmetry was seen on autopsy. In this patient, clinical evaluation revealed no asymmetric cortical symptoms, so the clinical diagnosis was Alzheimer disease. In the 13 cases with PSP, excluding 1 patient, no asymmetric atrophy was noted.

Atrophy of Midbrain Tegmentum

On midsagittal sections, by using the method of Oba et al,[2] the mean area of the midbrain tegmentum of the 4 patients with CBD was 67.6 ± 7.4 mm^2 (range, 62.3–73.3 mm^2) (Fig 3; case 1, Fig 4*A*–*D*), which is markedly less than normal, with the

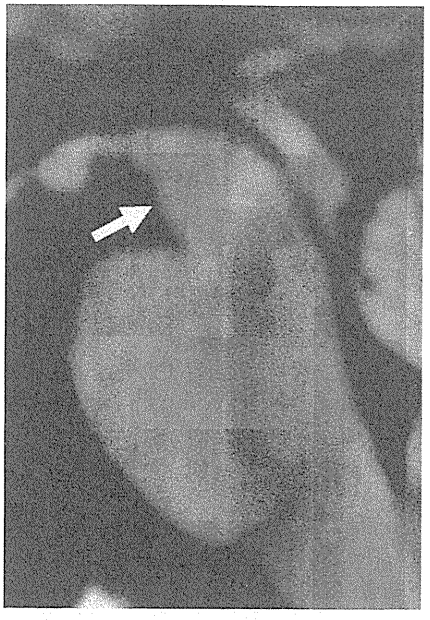

Fig 5. An age-matched healthy control 72-year-old woman. T1-weighted midsagittal image shows no obvious atrophy of the midbrain tegmentum (*arrow*). The area of the midbrain tegmentum is 128 mm^2.

Fig 6. Progressive supranuclear palsy. A 74-year-old man. T1-weighted midsagittal image clearly shows atrophy of the midbrain tegmentum (*arrow*). The area of the midbrain tegmentum is 71 mm^2.

mean area of 123.8 ± 10.8 mm^2 in the controls (range, 108.0–132.4 mm^2) (Figs 3 and 5). In the 13 patients with neuropathologically confirmed PSP, the mean area was 70.7 ± 12.1 mm^2 (range, 58.6–89.8 mm^2) (Figs 3 and 6). Although statistical analysis was not possible because of the small number of cases, there was no individual overlap of the midbrain tegmental area between the healthy controls and patients with CBD and PSP, apparently showing that severe atrophy of the midbrain tegmentum was present in CBD and PSP. On neuropathologic examination, there was also atrophy of the midbrain tegmentum and marked depigmentation of the substantia nigra and locus ceruleus. Other findings included melanophagia and gliosis, and Gallyas-Braak silver staining revealed argyrophilic threads and granular or fibrous inclusion bodies. These findings were consistent with CBD. In the pontine tegmentum and oculomotor and trochlear nuclei, many AT8-immunoreactive pretangles were observed.

SCWM Signa-Intensity Change on T2-Weighted Images and FLAIR

In all 4 patients with CBD, T2-weighted images and FLAIR showed diffuse high-intensity signals in the SCWM. In 3 patients, high signal intensity in the SCWM was recognized on the predominantly atrophic side (case 1, Fig 7*A*–*C*). In 1 patient, a high signal intensity was noted bilaterally over a wide area in the frontal lobes (case 3, Fig. 8*A*–*C*). Corresponding to the sites of white matter lesions, myelin sheath staining was decreased, and these sites were stained positively for antiphosphorylated tau antibody. These changes are primary characteristic of CBD. On neuropathologic examination, there was some involvement of U-fibers, but because of image-quality limitations on MR imaging, U-fiber involvement could not be specifically detected. In the 13 patients with PSP, there was no diffuse signal-intensity abnormality in the SCWM. There was no neuropathologic finding indicating primary degeneration of the SCWM.

Symmetric High Signal Intensity Bilaterally in Subthalamic Nuclei on T1-Weighted Images

T1-weighted MR images showed symmetric high signal intensity bilaterally in the subthalamic nuclei in all 3 patients in whom T1-weighted images were obtained (case 1, Fig 9*A*–*C*). In the remaining patient, the signal intensity in the subthalamic nuclei was not evaluated because no T1-weighted coronal spin-echo images could be obtained. Spoiled gradient echo (TR/TE, 21/6 ms; TI, 0 ms; flip angle, 20°) was selected instead. These sites showed a brownish change on macroscopic examination, and on microscopic examination, antiphosphorylated tau antibody–positive neurons and gliosis were observed. These changes were characteristic of CBD. MR imaging signal-intensity changes were also present in 4 of 7 patients with PSP in whom T1-weighted images were obtained (Fig 10*A*–*C*). Because neuropathologically examined cases were retrospectively evaluated, signal-intensity evaluation was limited to visual examination by 2 neuroradiologists. It was difficult to distinguish CBD and PSP on imaging, and no asymmetry was identified. However, on neuropathologic examination, degeneration of the subthalamic nuclei was more severe in PSP than in CBD.

Discussion

In 3 of the 4 patients with CBD, atrophy was predominantly contralateral and extended to the central sulcus. On neuropathologic examination, the MR imaging findings of atrophy were confirmed. In 1 patient with no asymmetric cortical symptoms, there was no asymmetry on MR imaging (case 2, Fig 3*A*, -*B*) and the clinical diagnosis was Alzheimer disease. In this patient, in whom the interval between the last MR imaging and autopsy was 3 years, neuropathologic examination did show asymmetric atrophy, but it was mild compared with that in the other 3 patients. In some patients, CBD presents with dementia, behavioral abnormalities, and attention deficit in

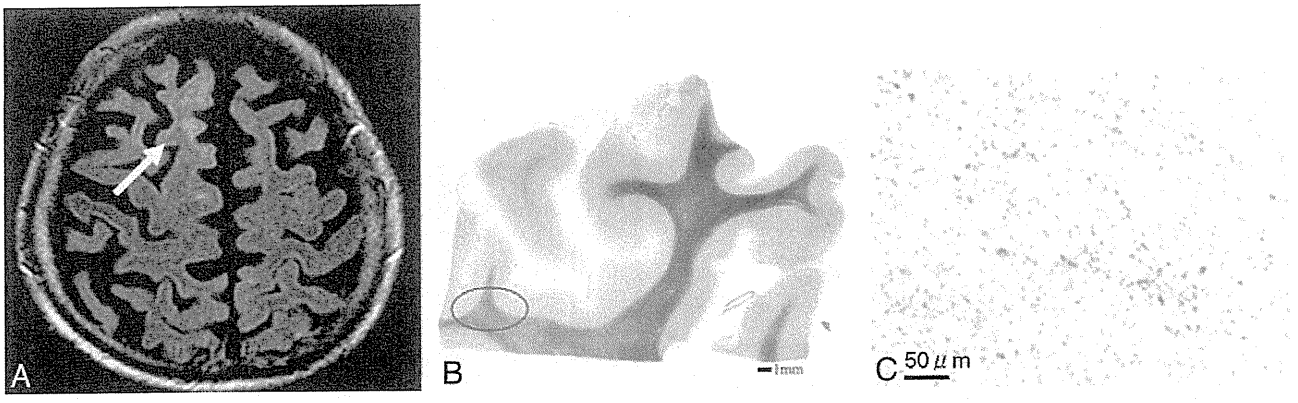

Fig 7. Corticobasal degeneration (CBD), case 1. An 84-year-old woman. *A*, Axial T2-weighted image shows a high signal intensity in the right frontal subcortical white matter (*white arrow*). *B*, In a microscopic specimen of the right frontal lobe corresponding to the site of white matter lesions, myelin sheath staining is decreased (*red oval*). The scale is 1 mm. *C*, In this area, there is positive staining for antiphosphorylated tau antibody on AT8 staining, which is compatible with the primary changes in CBD. The scale is 50 μm.

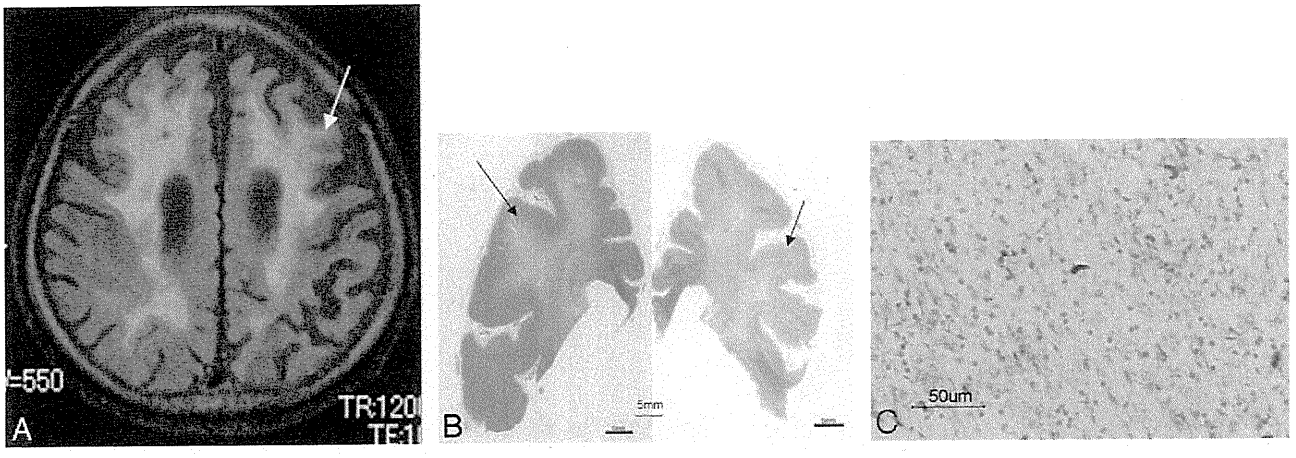

Fig 8. Corticobasal degeneration (CBD), case 3. A 70-year-old man. *A*, An axial fluid-attenuated inversion recovery image shows a high signal intensity bilaterally over a wide area in the frontal lobes (*arrow*). *B*, Corresponding to sites of white matter lesions, myelin sheath staining is decreased (*arrow*). The scale is 5 mm. *C*, These sites are stained positively for antiphosphorylated tau antibody. The scale is 50 μm. The changes are primary characteristics of CBD.

the early stage, but patients may be misdiagnosed due to a lack of cortical symptoms.[10-14] The above patient (case 2) may be an example of such a clinical presentation. Clinical evaluation showed little evidence of asymmetric cortical dysfunction, and neuropathology revealed only minimal cortical asymmetry. In this case, MR imaging showed a slight high signal intensity in the frontal SCWM; the midbrain tegmentum was severely atrophied, with an area of 71 mm^2; and T1-weighted imaging showed symmetric high-intensity signals in the subthalamic nucleus. Although a clear description is difficult on the basis of only 1 case, it was demonstrated by the pathologic findings that when identification of the cortical sign is difficult and unilateral atrophy is unclear on imaging, imaging findings, such as atrophy of the midbrain tegmentum, an abnormal signal intensity in the SCWM on FLAIR, or signal intensity changes in the subthalamic nuclei on T1-weighted imaging, may serve as supportive findings suggesting CBD.

CBD is important to differentiate from PSP. Oba et al[2] described a convenient and objective approach to diagnosing PSP based on midsagittal measurement of the midbrain tegmentum area. However, Koyama et al[1] also reported midbrain tegmentum atrophy in CBD. In our 4 cases of neuropathologically confirmed disease, severe midbrain tegmentum atrophy was also observed. Although there was a limited number of cases, because there was no individual overlap of the midbrain tegmental area between the healthy controls and patients with pathologically confirmed CBD and PSP, investigation of midbrain tegmental atrophy may have led to the diagnosis of CBD and PSP. Although no statistical analysis was performed because of the limited number of cases, it may be difficult to differentiate CBD from PSP on the basis of the presence of midbrain tegmental atrophy alone. A so-called "penguin sign" may be a distinguishing feature of PSP, but with severe midbrain tegmentum atrophy, both PSP and CBD must be considered. On neuropathology, there was marked depigmentation of the substantia nigra and locus ceruleus. Other findings included melanophagia and gliosis, and Gallyas-Braak silver staining revealed argyrophilic threads and granular or fibrous inclusion bodies. These findings were consistent with CBD as a cause of the atrophy. The degeneration of motor nerve nuclei, including the oculomotor and abducens nuclei, in the brain stem tegmentum was also noted, but no corresponding imaging findings were seen in the present study.

The localization of SCWM abnormalities, though different from those in previous reports,[1,15] was prominent in the present study. In CBD, Tokumaru et al,[15] Doi et al,[16] and Koyama et al[1] described predominantly unilateral SCWM abnormalities on T2-weighted imaging and FLAIR. In their re-

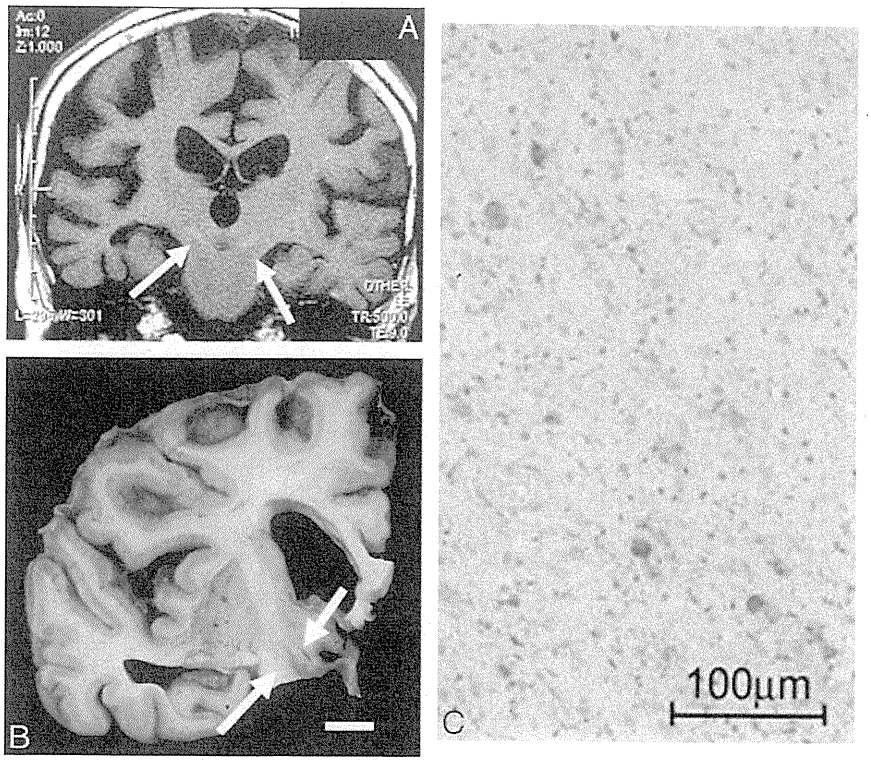

Fig 9. Corticobasal degeneration (CBD), case 1. An 84-year-old woman. *A*, Coronal T1-weighted image shows symmetric high signal intensity bilaterally in the subthalamic nuclei (*arrows*). *B*, A macroscopic specimen shows a brownish change in the subthalamic nuclei (*arrows*). *C*, On microscopic examination (AT8 stain), antiphosphorylated tau antibody–positive neurons and gliosis are observed. These changes are characteristic of CBD. The scale is 100 μm.

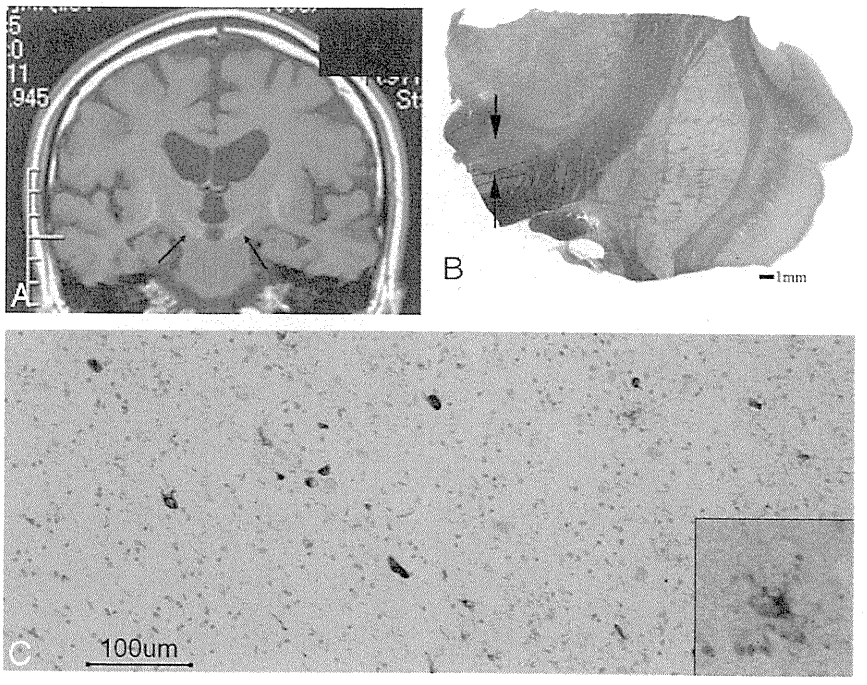

Fig 10. Progressive supranuclear palsy (PSP). An 84-year-old man. *A*, Coronal T1-weighted image shows a symmetric high signal intensity bilaterally in the subthalamic nuclei (*arrow*). *B*, A microscopic specimen of myelin-sheath staining shows the atrophic change of the subthalamic nuclei (*arrows*). The scale is 1 mm. *C*, On microscopic examination in the subthalamic nuclei, AT8 staining is clearly positive in the neurons (brown area). An enlarged image shows a tuft. These changes are characteristic of PSP. The scale is 100 μm.

ports, localization in the precentral gyrus of the SCWM and signal-intensity abnormalities contralateral to the clinically affected side were noted.[1,15] However, in the present study, the localization of white matter signal-intensity abnormalities differed among the 3 cases. In particular, in case 3, T2-weighted imaging and FLAIR showed widespread signal-intensity changes in the frontal lobe white matter bilaterally. This appearance differed from that reported by Doi et al[16] and Koyama et al.[1] In 2 patients, signal-intensity abnormalities were present in the superior frontal gyrus white matter. Only 1

patient showed signal-intensity abnormalities in the precentral gyrus SCWM. It is important to recognize the possibility of CBD showing different localizations of atrophy and white matter signal-intensity abnormalities rather than findings in the more typical cases as reported by Koyama et al.[1] In cases without predominantly unilateral cortical signs on clinical evaluation, the localization of atrophy and SCWM signal-intensity abnormalities may differ from typical cases. In these cases, MR imaging findings of high signal intensity in the subthalamic nucleus on T1-weighted images and severe atrophy of the midbrain tegmentum on midsagittal sections can provide useful information.

Rebeiz et al[17] first reported CBD with distinct features and a clinically asymmetric onset characterized by apraxia, dystonia, postural instability, and an akinetic-rigid syndrome that does not respond to levodopa, but since then, cases presenting with dementia, in which Alzheimer or Pick disease must be ruled out, and cases with other clinical features, in which PSP must be ruled out, have been reported.[18-21] A variety of underlying neuropathologic features have also been reported. Recent reports clarified the presence of many phenotypes of CBD neuropathologically and clinically.[10-14] Although there were only 4 cases, it was difficult to diagnose CBD clinically in cases definitely diagnosed neuropathologically, and 1 case showed imaging findings different from those previously reported. The lesions in the white matter widely expanded bilaterally in case 3, indicating that the clinical features alone did not confirm CBD. This case probably represents a new clinical phenotype of CBD.

Neuropathologic examination of SCWM lesions that correlated with the MR imaging findings showed the typical tauopathy of CBD. The degenerative changes were characteristic of CBD. In 1996, we suggested, on the basis of the neuropathologic findings in CBD, that white matter lesions of the frontal lobe were secondary degenerative changes.[15] Doi et al[16] and Koyama et al[1] also believe that these white matter lesions in CBD reflect the progression of neuronal degeneration, especially demyelination secondary to axonal loss or change. However, in the present study, at sites where MR imaging showed white matter lesions, though neuropathologic examination revealed some secondary degeneration, tauopathy in the white matter, particularly the SCWM, was clearly evident. This shows a positive radio-pathologic correlation of these changes in CBD. In 2002, Dickson et al[8] proposed neuropathologic criteria, with a primary emphasis on tau-positive neuronal and glial lesions, for the diagnosis of CBD. Advances in neuropathologic staining methods to evaluate tau have expanded our knowledge of these primary changes in CBD. Dickson et al also confirmed tauopathy of the white matter in CBD. After the report of Dickson et al, the neuropathologic evaluation criteria for lesions in the white matter apparently changed, and the finding that lesions in the white matter were primary degeneration in CBD, not secondary, may be important new information for the evaluation of an association with clinical and pathologic findings. In the present cases, degeneration was severe, affecting U-fibers, which should be investigated to collate with MR images.

T1-weighted images, obtained in 3 patients with CBD, showed symmetric high-intensity signals in the subthalamic nucleus. This finding was also present in a high proportion of patients with PSP, making an MR imaging–based differential diagnosis difficult. Neuropathology of sites corresponding to these signal-intensity changes showed tauopathy-related degeneration. Gliosis was also present, but on T2-weighted imaging and FLAIR, signal-intensity changes were difficult to detect. Only axial sections were obtained on T2-weighted imaging. These may have been insufficient to delineate the subthalamic nucleus adequately. In PSP, there was a high rate of similar findings, so these were not useful in the differential diagnosis. In all patients with PSP, the neuropathology showed more severe degeneration than in those with CBD. In addition to midbrain tegmentum atrophy, the localization of degeneration was similar in CBD to that seen in PSP. These signal-intensity changes were only visually evaluated by the neuroradiologists in the limited number of cases, but no signal-intensity change was noted in the pathologically healthy group, suggesting that primary degenerative findings of the individual diseases in the subthalamic nuclei and abnormal signals in this region are significant to some extent. However, differentiating CBD and PSP based on these findings alone is not possible. Therefore, a combination of imaging findings, including the presence of white matter signal-intensity changes and asymmetric atrophy, is important in correctly diagnosing CBD.

Conclusions

The correlation between radiologic and pathologic findings was investigated in patients with CBD, and MR imaging findings that could be used to differentiate CBD from PSP clinically were identified.

In CBD, midbrain tegmentum atrophy was severe, and degeneration in this area was correlated with the severity. However, this finding did not help in the differential diagnosis distinguishing CBD from PSP. T1-weighted imaging showed symmetric high-intensity signals in the subthalamic nucleus, but a large proportion of patients with PSP had a similar finding. On neuropathologic examination, each disorder showed characteristic degeneration. The degree of degeneration was more severe in PSP, but no imaging-based differences were observed. In CBD, there was a high rate of atrophy contralateral to the clinically affected side, with extension to the central sulcus. This suggests that the localization of atrophy differs depending on the underlying etiology. In PSP, unilateral atrophy was not a predominant finding.

MR imaging, FLAIR, and T2-weighted imaging showed high signal intensities in the SCWM. Previous studies have correlated this finding with secondary degeneration. The present study is the first to correlate these SCWM signal-intensity changes with primary degeneration in CBD. In addition, the localization of white matter lesions was correlated with a variety of clinical phenotypes. This suggests that there are CBD types other than those that are localized only to the precentral gyrus SCWM.

References

1. Koyama M, Yagishita A, Nakata Y, et al. **Imaging of corticobasal degeneration syndrome.** *Neuroradiology* 2007;49:905–12
2. Oba H, Yagishita A, Terada H, et al. **New and reliable MRI diagnosis for progressive supranuclear palsy.** *Neurology* 2005;28:2050–55
3. Saito Y, Murayama S. **Neuropathology of mild cognitive impairment.** *Neuropathology* 2007;27:578–84
4. Mirra SS, Heyman A, McKeel D, et al. **The Consortium to Establish a Registry**

for Alzheimer's Disease (CERAD). Part II. Standardization of the neuropathologic assessment of Alzheimer's disease. *Neurology* 1991;41:479–86
5. Saito Y, Ruberu NN, Sawabe M, et al. **Lewy body-related alpha-synucleinopathy in aging.** *J Neuropathol Exp Neurol* 2004;63:742–49
6. McKeith IG, Galasko D, Kosaka K, et al. **Consensus guidelines for the clinical and pathologic diagnosis of dementia with Lewy bodies (DLB): report of the consortium on DLB international workshop.** *Neurology* 1996;47:1113–24
7. Braak H, Braak E. **Neuropathological stageing of Alzheimer-related changes.** *Acta Neuropathol* 1991;82:239–59
8. Dickson DW, Bergeron C, Chin SS, et al. **Office of Rare Diseases Neuropathologic Criteria for corticobasal degeneration.** *J Neuropathol Exp Neurol* 2002;61:935–46
9. Hauw JJ, Daniel SE, Dickson D, et al. **Preliminary NINDS neuropathologic criteria for Steele-Richardson-Olszewski syndrome (progressive supranuclear palsy).** *Neurology* 1994;44:2015–19
10. Mathuranath PS, Xuereb JH, Bak T, et al. **Corticobasal ganglionic degeneration and/or frontotemporal dementia? A report of two overlap cases and review of literature.** *J Neurol Neurosurg Psychiatry* 2000;68:304–12
11. Grimes DA, Lang AE, Bergeron CB. **Dementia as the most common presentation of cortical-basal ganglionic degeneration.** *Neurology* 1999;53:1969–74
12. Schneider JA, Watts RL, Gearing M, et al. **Corticobasal degeneration: neuropathologic and clinical heterogeneity.** *Neurology* 1997;48:959:969
13. Rinne JO, Lee MS, Thompson PD, et al. **Corticobasal degeneration: a clinical study of 36 cases.** *Brain* 1994;117:1183–96
14. Bergeron C, Pollanen MS, Weyer L, et al. **Unusual clinical presentations of cortical-basal ganglionic degeneration.** *Ann Neurol* 1996;40:893–900
15. Tokumaru AM, O'uchi T, Kuru Y, et al. **Corticobasal degeneration: MR with histopathologic comparison.** *AJNR Am J Neuroradiol* 1996;17:1849–52
16. Doi T, Iwasa K, Makifuchi T, et al. **White matter hyperintensities on MRI in a patient with corticobasal degeneration.** *Acta Neurol Scand* 1999;99:199–201
17. Rebeiz JJ, Kolodny EH, Richardson EP Jr. **Corticodentatonigral degeneration with neuronal achromasia: a progressive disorder of late adult life.** *Trans Am Neurol Assoc* 1967;92:23–26
18. Brown J, Lantos PL, Roques P, et al. **Familial dementia with swollen achromatic neuron and corticobasal inclusion bodies: a clinical and pathological study.** *J Neurol Sci* 1996;135:21–30
19. Doran M, du Plessis DG, Enevoldson TP, et al. **Pathological heterogeneity of clinically diagnosed corticobasal degeneration.** *J Neurol Sci* 2003;216:127–34
20. Feany MB, Mattiace LA, Dickson DW. **Neuropathologic overlap of progressive supranuclear palsy, Pick's disease, and corticobasal degeneration.** *J Neuropathol Exp Neurol* 1996;55:53–67
21. Jendroska K, Rossor MN, Mathias CJ, et al. **Morphological overlap between corticobasal degeneration and Pick's disease: a clinicopathological report.** *Mov Disord* 1995;10:111–14

Eur J Nucl Med Mol Imaging (2010) 37:3–11
DOI 10.1007/s00259-009-1202-1

ORIGINAL ARTICLE

Validation of cardiac ^{123}I-MIBG scintigraphy in patients with Parkinson's disease who were diagnosed with dopamine PET

Kenji Ishibashi · Yuko Saito · Shigeo Murayama · Kazutomi Kanemaru · Keiichi Oda · Kiichi Ishiwata · Hidehiro Mizusawa · Kenji Ishii

Received: 11 March 2009 / Accepted: 9 June 2009 / Published online: 22 July 2009

Abstract
Purpose The aim of this study was to evaluate the diagnostic potential of cardiac ^{123}I-labelled metaiodobenzylguanidine (^{123}I-MIBG) scintigraphy in idiopathic Parkinson's disease (PD). The diagnosis was confirmed by positron emission tomography (PET) imaging with ^{11}C-labelled 2β-carbomethoxy-3β-(4-fluorophenyl)-tropane (^{11}C-CFT) and ^{11}C-raclopride (together designated as dopamine PET).
Methods Cardiac ^{123}I-MIBG scintigraphy and dopamine PET were performed for 39 parkinsonian patients. To estimate the cardiac ^{123}I-MIBG uptake, heart to mediastinum (H/M) ratios in early and delayed images were calculated. On the basis of established clinical criteria and our dopamine PET findings, 24 patients were classified into the PD group and 15 into the non-PD (NPD) group.
Results Both early and delayed images showed that the H/M ratios were significantly lower in the PD group than in the NPD group. When the optimal cut-off levels of the H/M ratio were set at 1.95 and 1.60 in the early and delayed images, respectively, by receiver-operating characteristic analysis, the sensitivity of cardiac ^{123}I-MIBG scintigraphy for the diagnosis of PD was 79.2 and 70.8% and the specificity was 93.3 and 93.3% in the early and delayed images, respectively. In the Hoehn and Yahr 1 and 2 PD patients, the sensitivity decreased by 69.2 and 53.8% in the early and delayed images, respectively.
Conclusion In early PD cases, cardiac ^{123}I-MIBG scintigraphy is of limited value in the diagnosis, because of its relatively lower sensitivity. However, because of its high specificity for the overall cases, cardiac ^{123}I-MIBG scintigraphy may assist in the diagnosis of PD in a complementary role with the dopaminergic neuroimaging.

Keywords ^{123}I-MIBG · ^{11}C-CFT · ^{11}C-Raclopride · Scintigraphy · Positron emission tomography · Parkinson's disease

An Editorial Commentary on this paper is available at http://dx.doi.org/10.1007/s00259-009-1215-9.

K. Ishibashi · H. Mizusawa
Department of Neurology and Neurological Science,
Graduate School, Tokyo Medical and Dental University,
Tokyo, Japan

K. Ishibashi · K. Oda · K. Ishiwata · K. Ishii (✉)
Positron Medical Center,
Tokyo Metropolitan Institute of Gerontology,
1-1 Nakacho, Itabashi-ku,
Tokyo 173-0022, Japan
e-mail: ishii@pet.tmig.or.jp

Y. Saito
Department of Pathology, Tokyo Metropolitan Geriatric Hospital,
Tokyo, Japan

Y. Saito · S. Murayama
Department of Neuropathology,
Tokyo Metropolitan Institute of Gerontology,
Tokyo, Japan

K. Kanemaru
Department of Neurology, Tokyo Metropolitan Geriatric Hospital,
Tokyo, Japan

Introduction

Cardiac ^{123}I-labelled metaiodobenzylguanidine (^{123}I-MIBG) scintigraphy has been suggested to be useful for the diagnosis of idiopathic Parkinson's disease (PD), because many recent studies have revealed that cardiac ^{123}I-MIBG uptake decreases with disease progression and that almost all

patients in the advanced stage of PD show decreased cardiac ^{123}I-MIBG uptake [1–5]. However, it is unclear whether cardiac ^{123}I-MIBG uptake is a good surrogate marker for the diagnosis of PD, especially in early and mild PD cases, which are the most difficult to diagnose in daily clinical practice, because the data on the reduction of cardiac ^{123}I-MIBG uptake in the early stage of PD vary greatly among different studies [1–8]. Therefore, we aimed to investigate the sensitivity and specificity of cardiac ^{123}I-MIBG scintigraphy in diagnosing PD, focusing on early and mild cases of PD in the Hoehn and Yahr (HY) stages 1 and 2.

While planning this study, we focused on dividing the patients into PD and non-PD (NPD) groups in the most appropriate manner in order to acquire precise results. Previous studies have shown that the usual clinical diagnostic accuracy of PD ranges from 70 to 90%, and the accuracy rate greatly decreases in early cases [9–12]. In vivo neurofunctional imaging of the basal ganglia, which provides images of both pre- and postsynaptic nigrostriatal dopaminergic functions, has been recognized as a standard marker for the diagnosis of PD in every clinical stage [13–25]. Therefore, in order to improve the accuracy of the diagnosis of PD, especially in early PD cases, and to classify the patients into the PD and NPD groups in a more appropriate manner, we performed positron emission tomography (PET) imaging with ^{11}C-labelled 2β-carbomethoxy-3β-(4-fluorophenyl)-tropane (^{11}C-CFT) and ^{11}C-raclopride. PET imaging with ^{11}C-CFT and ^{11}C-raclopride can assess the levels of presynaptic dopamine transporter (DAT) and postsynaptic dopamine D_2-like receptor (D_2R), respectively, in the striatum. The two types of PET imaging techniques were together designated as dopamine PET. Further, we proposed the definitions of PD and NPD patterns in dopamine PET findings on the basis of the results which had been confirmed by previous studies.

We also investigated the association between cardiac sympathetic function assessed by cardiac ^{123}I-MIBG uptake, presynaptic nigrostriatal dopaminergic function assessed by striatal ^{11}C-CFT uptake and disease stage determined according to the HY scale.

Materials and methods

Subjects

The present study was a retrospective study. The subjects comprised 39 patients who visited the neurological outpatient clinic at Tokyo Metropolitan Geriatric Hospital from November 2001 to October 2007. They chiefly complained of one or more parkinsonian symptoms, including resting tremor, rigidity, bradykinesia and postural instability. The patients were divided into PD and NPD groups (Fig. 1). Cardiac ^{123}I-MIBG scintigraphy, dopamine PET and magnetic resonance imaging (MRI) were performed for all patients. None of the patients had any concomitant hereditary disorder that could cause parkinsonian symptoms. None of the patients had an individual history of any heart disease. Further, none of the patients were on any medication that could cause parkinsonian symptoms.

For dopamine PET, eight healthy subjects (five men and three women) aged 55–74 years [mean±standard deviation (SD) = 62.3±6.9 years)]were considered as controls. They were deemed healthy based on their medical history, physical and neurological examinations and MRI of the brain. Further, none of them were on medication.

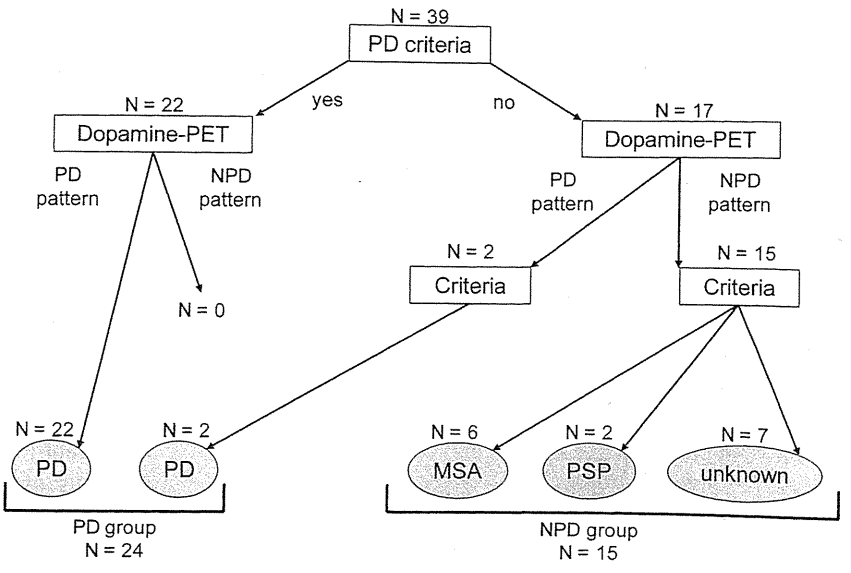

Fig. 1 Diagnostic flow chart and schematic representation of classification process. Patients were classified into PD and NPD groups on the basis of respective published clinical criteria and our dopamine PET findings

This study protocol was approved by the Ethics Committee of the Tokyo Metropolitan Institute of Gerontology. Written informed consent was obtained from all participants.

PET imaging

PET imaging was performed at the Positron Medical Center, Tokyo Metropolitan Institute of Gerontology by using a SET-2400 W scanner (Shimadzu, Kyoto, Japan) in the three-dimensional scanning mode [26], as described previously [27, 28]. The transmission data were acquired using a rotating ^{68}Ga/^{68}Ge rod source for attenuation correction. Images of 50 slices were obtained with a resolution of 2×2×3.125 mm voxels and a 128×128 matrix.

Dopamine PET imaging ^{11}C-CFT and ^{11}C-raclopride were prepared as described previously [29, 30]. The two types of PET imaging were performed for all of the subjects on the same day. The patients being treated with antiparkinsonian drugs underwent dopamine PET following at least 15 h deprivation of the medications. Each subject was administered an intravenous bolus injection of 341±62 (mean ± SD) MBq of ^{11}C-CFT, followed by that of 311±56 (mean ± SD) MBq of ^{11}C-raclopride after 2.5–3 h. To measure the uptake of the tracers, static scanning was performed for 75–90 and 40–55 min after the injection of ^{11}C-CFT and ^{11}C-raclopride, respectively. The specific activity of ^{11}C-CFT and ^{11}C-raclopride at the time of injection ranged from 5.9 to 134.2 GBq/μmol and from 10.2 to 201.7 GBq/μmol, respectively.

Analysis of dopamine PET images Image manipulations were performed using Dr. View version R2.0 (AJS, Tokyo, Japan) and SPM2 (Functional Imaging Laboratory, London, UK) implemented in MATLAB version 7.0.1 (The MathWorks, Natick, MA, USA).

The two PET images and one MRI image obtained for each subject were coregistered. The three coregistered images were resliced transaxially, parallel to the anteroposterior intercommissural (AC-PC) line. Circular regions of interest (ROIs) were selected with reference to the brain atlas and individually coregistered MRI images. In each of the three contiguous slices, one ROI with 8-mm diameter was selected on the caudate, two ROIs on the anterior putamen and two on the posterior putamen on both the left and right sides. In other words, the AC-PC plane and regions 3.1 and 6.2 mm above the AC-PC line were selected. A total of 50 ROIs with 10-mm diameter were selected throughout the cerebellar cortex in five contiguous slices.

To evaluate the uptake of ^{11}C-CFT and ^{11}C-raclopride, we calculated the uptake ratio index by the following formula [15, 31]: uptake ratio index = (activity in each region − activity in the cerebellum)/(activity in the cerebellum). We previously validated the method to estimate the binding potential of ^{11}C-raclopride and ^{11}C-CFT, adopting the uptake ratio index [27, 28]. For the further analyses, the uptake of each tracer in each subregion of the striatum (the caudate, anterior putamen and posterior putamen) was evaluated as the average value of the left and right sides. The uptake of each tracer in the whole striatum was evaluated as the average value of entire ROIs in the whole striatum.

Cardiac ^{123}I-MIBG scintigraphy

Scintigraphic studies were performed at Tokyo Metropolitan Geriatric Hospital by using a triple-headed gamma camera (PRISM-3000, Shimadzu, Kyoto, Japan). None of the patients were on any medication, i.e. they were not receiving any drugs such as antidepressants and monoamine oxidase inhibitors, which might influence cardiac ^{123}I-MIBG uptake. After a 30-min resting period, each patient was administered an intravenous bolus injection of 111 MBq of ^{123}I-MIBG (Fujifilm RI Pharma Co., Tokyo, Japan). Planar images of the chest in the anterior view were obtained twice for 5 min, starting at 20 min (early phase) and then at 180 min (delayed phase) after the injection of ^{123}I-MIBG. Relative organ uptake of ^{123}I-MIBG was determined by selecting the ROIs on the heart and mediastinum in the anterior planar image [32]. Average counts per pixel in the heart and mediastinum were used to calculate the heart to mediastinum (H/M) ratio.

MRI

MRI was performed at Tokyo Metropolitan Geriatric Hospital. By using a 1.5-T Signa EXCITE HD scanner (GE, Milwaukee, WI, USA), transaxial T1-weighted images [three-dimensional spoiled gradient-recalled (3D SPGR), repetition time (TR) = 9.2 ms, echo time (TE) = 2.0 ms, matrix size = 256 × 256 × 124, voxel size = 0.94 × 0.94 × 1.3mm] and transaxial T2-weighted images (first spin echo, TR= 3,000 ms, TE=100 ms, matrix size = 256 × 256 × 20, voxel size = 0.7 × 0.7 × 6.5mm) were obtained.

Clinical diagnosis

The diagnostic flow chart is shown in Fig. 1. First, the patients were divided into two groups (22 patients in one group and 17 patients in the other) on the basis of the clinical criteria of the UK Parkinson's Disease Brain Bank (UKPDBB) [10]. Each group was then further classified on the basis of dopamine PET findings. As shown in Fig. 2, the PD pattern in dopamine PET was defined as follows: (1)

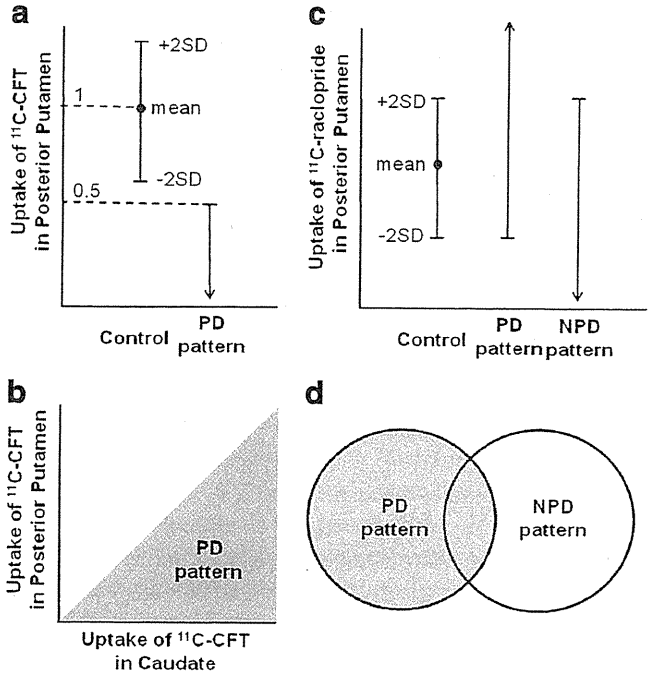

Fig. 2 PD and NPD patterns defined on the basis of dopamine PET findings. PD pattern: ^{11}C-CFT uptake in the posterior putamen of patients less than 50% of the mean uptake in the posterior putamen of normal controls (**a**) and less than that in the caudate of patients (**b**); ^{11}C-raclopride uptake in the posterior putamen of patients more than the mean – 2 SD of the uptake in the posterior putamen of normal controls (**c**). NPD pattern: ^{11}C-raclopride uptake in the posterior putamen of patients less than the mean + 2 SD of the uptake in the posterior putamen of normal controls (**c**). The patient was considered to be PD pattern when both PD and NPD were fulfilled (**d**). The uptake in each subregion of the striatum was evaluated as the average value of both sides

^{11}C-CFT uptake in the posterior putamen of the patients less than 50% of the mean uptake in the posterior putamen of normal controls (Fig. 2a) and less than that in the caudate of the patients (Fig. 2b) and (2) ^{11}C-raclopride uptake in the posterior putamen of the patients more than the mean – 2 SD of the uptake in the posterior putamen of normal controls (Fig. 2c). The NPD pattern was defined as follows: ^{11}C-raclopride uptake in the posterior putamen of the patients less than the mean + 2 SD of the uptake in the posterior putamen of normal controls (Fig. 2c). The patient was considered to be PD pattern when both PD and NPD were fulfilled (Fig. 2d).

Statistical analysis

Differences in the averages and variances were tested by Student's *t* test and one-way analysis of variance, respectively. Correlations between the two groups of patients were assessed by linear regression analysis with Pearson's correlation test; *p* values of <0.05 were considered statistically significant.

Results

Patients

Classification into PD and NPD groups All 22 patients who fulfilled the UKPDBB PD criteria at initial diagnosis [10] showed the PD pattern on dopamine PET (Fig. 1). They were classified into the PD group. The other 17 patients were further classified according to dopamine PET findings and respective published clinical criteria. Of the 17 patients, 2 showed the PD pattern on dopamine PET. In fact, the symptom manifested was only resting tremor at initial diagnosis; however, during the course of the study, they fulfilled the UKPDBB PD criteria [10] and were classified into the PD group.

Of the 17 patients, 15 showed the NPD pattern on dopamine PET and were classified into the NPD group (Fig. 1). These patients were then further divided into three subgroups. Six patients fulfilled the multiple system atrophy (MSA) criteria [33]. Two patients fulfilled the progressive supranuclear palsy (PSP) criteria [34]. For the remaining seven patients, no definitive diagnoses could be established despite follow-up for more than 1 year.

Finally, 24 patients (7 men and 17 women, age range: 60–85 years, mean age ± SD = 71.5±6.8 years) and 15 patients (8 men and 7 women, age range: 65–86 years, mean age ± SD: 76.0±5.5 years) were classified into the PD and NPD groups, respectively.

Demographic data Patient characteristics are summarized in Table 1. In the PD group, 11 patients were drug naive, 7 were being treated with L-dopa and 6 were being treated with L-dopa and dopamine agonists at the time of dopamine PET. The interval between cardiac ^{123}I-MIBG scintigraphy and dopamine PET was within 6 months for 16 patients, between 6 and 12 months for 1 patient and more than 1 year for 7 patients. However, the HY stage of each patient in the PD group remained the same between cardiac ^{123}I-MIBG scintigraphy and dopamine PET. In the NPD group, 11 patients were not administered any antiparkinsonian drug, and 4 were being treated with only L-dopa. The interval between the two examinations was within 6 months for 12 patients, between 6 and 12 months for 1 patient and more than 1 year for 2 patients.

Uptake of ^{123}I-MIBG

Both the early and delayed images showed significantly lower H/M ratios in the PD group than in the NPD group (Fig. 3). In both the early and delayed images, the H/M ratios tended to decrease with the progression of the HY stages; however, the decrease was not statistically significant.

Table 1 Clinical features of patients in Parkinson's disease and non-Parkinson's disease groups

Groups	Patients		Age (years)	Duration (years)	^{123}I-MIBG scintigraphy		^{11}C-CFT PET
	Number	M:F			Heart to mediastinum ratio		Uptake ratio index in the whole striatum
					Early	Delayed	
Parkinson's disease	24	7:17	71.5±6.8	3.5±3.2	1.66±0.45	1.46±0.41	0.98±0.34
Hoehn and Yahr 1	4	0:4	65.0±7.7	2.9±2.6	1.75±0.33	1.49±0.29	1.49±0.40
Hoehn and Yahr 2	9	2:7	73.9±5.6	2.4±1.0	1.81±0.54	1.60±0.45	1.00±0.20
Hoehn and Yahr 3	8	5:3	71.9±7.2	3.0±1.8	1.57±0.44	1.41±0.44	0.81±0.20
Hoehn and Yahr 4	3	0:3	72.3±5.0	9.0±6.1	1.36±0.05	1.12±0.08	0.69±0.07
Non-Parkinson's disease	15	8:7	76.0±5.5	2.8±1.9	2.35±0.46	2.18±0.51	1.65±0.68

Data are expressed as mean±SD

Table 2 shows the sensitivity and specificity of cardiac ^{123}I-MIBG scintigraphy in differentiating patients with PD from the other patients with chief complaints of parkinsonian symptoms. When the optimal cut-off levels of ^{123}I-MIBG were set at 1.95 and 1.60 by receiver-operating characteristic analysis, the sensitivity of cardiac ^{123}I-MIBG scintigraphy for the diagnosis of PD was 79.2 and 70.8% and the specificity was 93.3 and 93.3% in the early image and delayed images, respectively. In HY 1 and 2 PD patients the sensitivity was 69.2 and 53.9% and in HY 3 and 4 PD patients the sensitivity was 90.9 and 90.9% in the early image and delayed images, respectively

Uptake of ^{11}C-CFT

The uptake of ^{11}C-CFT in the whole striatum decreased with the progression of the HY stages (Fig. 4). Significant reduction in the ^{11}C-CFT uptake with the progression of the HY stages was also observed in each of the three subregions of the striatum. Correlation between cardiac ^{123}I-MIBG scintigraphy and ^{11}C-CFT PET was evaluated in the 16 patients who underwent the two examinations within 6 months. There was no significant correlation between the ^{11}C-CFT uptake in the whole striatum and the H/M ratios in both the early images (r=0.15, p=0.59) and delayed images (r=0.21, p=0.43) (Fig. 5). Further, no significant correlation was observed between the ^{11}C-CFT uptake in each of the three subregions of the striatum and the H/M ratio.

Discussion

In the present study, we investigated the sensitivity and specificity of cardiac ^{123}I-MIBG scintigraphy in diagnosing PD and differentiating the patients with PD from the others with chief complaints of parkinsonian symptoms. Further, we investigated the correlation between cardiac sympathetic function assessed by cardiac ^{123}I-MIBG uptake, nigrostriatal

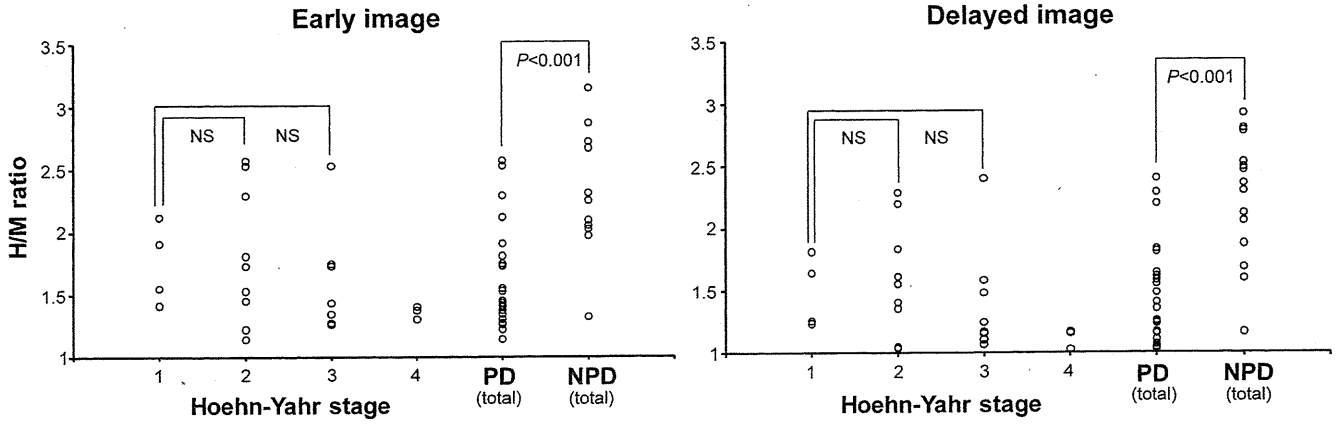

Fig. 3 H/M ratios in the PD and NPD groups in early and delayed images. Each graph represents the relation between the H/M ratio and Hoehn and Yahr stage of PD and a comparison of the H/M ratios of the total number of PD and NPD patients. Both images showed that the H/M ratios were significantly lower in the PD group than in the NPD group; however, the H/M ratios of patients in HY 1 of PD were not significantly higher than those of the patients in HY 2 and 3 of PD. *NS* not significant

Table 2 Sensitivity and specificity of cardiac ^{123}I-MIBG scintigraphy in differentiating Parkinson's disease from other parkinsonian syndromes

Total PD patients (n=24)												
	Early image						Delayed image					
Cut-off	1.80	1.85	1.90	1.95	2.00	2.05	1.60	1.65	1.70	1.75	1.80	1.85
Sensitivity	70.8%	75.0%	75.0%	79.2%	79.2%	79.2%	70.8%	75.0%	79.2%	79.2%	79.2%	87.5%
Specificity	93.3%	93.3%	93.3%	93.3%	86.7%	80.0%	93.3%	80.0%	73.3%	73.3%	73.3%	73.3%
Hoehn and Yahr 1 and 2 (n=15)												
	Early image						Delayed image					
Cut-off	1.80	1.85	1.90	1.95	2.00	2.05	1.60	1.65	1.70	1.75	1.80	1.85
Sensitivity	53.8%	61.5%	61.5%	69.2%	69.2%	69.2%	53.8%	61.5%	69.2%	69.2%	69.2%	84.6%

Cut-off levels, for which both the sensitivity and specificity were more than 70%, are shown. The optimal cut-off levels determined by receiver-operating characteristic analysis were at 1.95 and 1.60 in the early and delayed images, respectively

dopaminergic function assessed by ^{11}C-CFT uptake and disease stage determined according to the HY scale.

It has been reported that cardiac ^{123}I-MIBG uptake in patients with PD is significantly lower than that in patients with other parkinsonian syndromes [1–7]; this result corresponds to our results. Several reports suggest that the severity of motor impairment and disease duration are correlated with reduced ^{123}I-MIBG uptake in patients with PD [1, 2, 5, 6]; however, some other findings deny such correlations, similar to ours [3, 4, 7, 8]. This discrepancy is presumably explained by the fact that the degree of cardiac ^{123}I-MIBG uptake in patients in HY 1 and 2 of PD varies greatly among different studies. Difficult definitive diagnosis of PD in early and mild cases may also be because of the great variation. On the other hand, almost all patients in the advanced stage of PD have shown very low ^{123}I-MIBG uptake in both the previous and the present studies. Li et al. reported that cardiac sympathetic denervation progresses over time and that the rate of decrease in the number of sympathetic terminals appears to be at least as high as that of nigrostriatal dopaminergic terminals [35]. Therefore, we considered that although the onset of cardiac sympathetic denervation varied among the patients with PD, severe cardiac sympathetic denervation occurred in all of the patients by the terminal stage of PD. In regard to the association with a sympathetic symptom, it was reported that reduced ^{123}I-MIBG uptake does not always mean the existence of a sympathetic symptom [1, 3, 4, 7]. Also in this study, of the three patients in stage 4 of the HY scale who showed very low ^{123}I-MIBG uptake (Fig. 3), two had orthostatic hypotension; however, the remaining one patient had no cardiovascular sympathetic symptom and showed no abnormality in the head-up tilt test. In contrast to ^{123}I-MIBG uptake, the decrease in ^{11}C-CFT uptake in the whole striatum and in each of its three subregions significantly correlated with disease progression represented by the HY stages, as reported previously [14, 16, 22]. Considering the causal pathophysiological mechanism of PD, this is reasonable because ^{11}C-CFT uptake directly indicates nigrostriatal dopaminergic function.

We investigated the sensitivity and specificity of cardiac ^{123}I-MIBG scintigraphy in diagnosing PD and differentiating the patients with PD from the other patients with chief complaints of parkinsonian symptoms. Similar to the

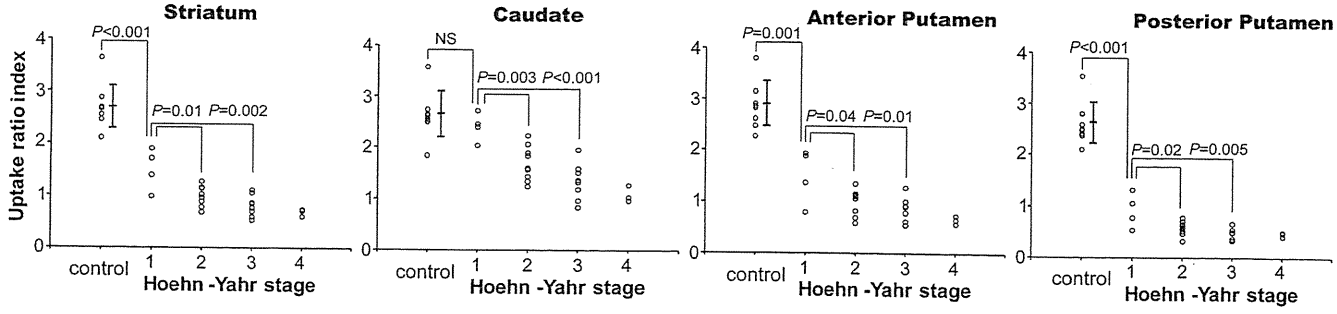

Fig. 4 Relation between the HY stage and uptake ratio index of ^{11}C-CFT in the whole striatum, caudate, anterior putamen and posterior putamen of patients with PD. In all four graphs, the uptakes in the patients in HY 1 of PD are significantly higher than those in the patients in HY 2 and 3 of PD. The uptakes in the caudate of patients in HY 1 of PD are not significantly higher than those in the caudate of controls, while the uptakes in the whole striatum, anterior putamen and posterior putamen of patients in HY 1 of PD are significantly higher than those in the corresponding regions of the controls. The *vertical bar* represents the mean ± SD of controls. *NS* not significant

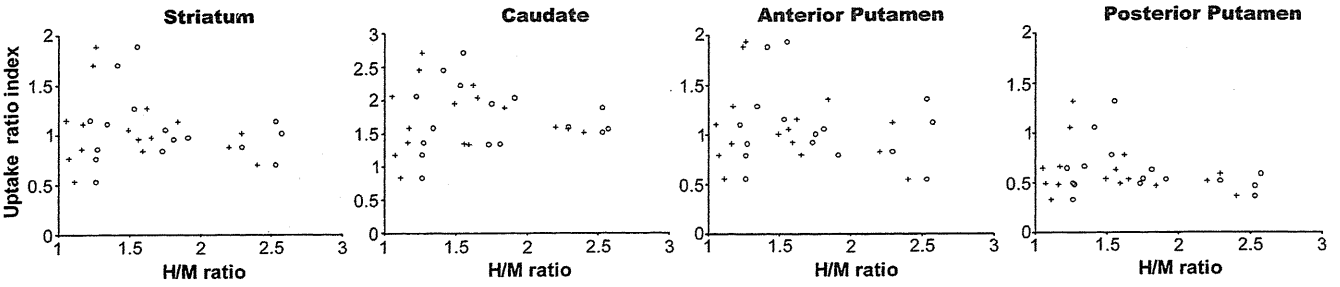

Fig. 5 Relation between the H/M ratio and uptake ratio index of ^{11}C-CFT in the whole striatum, caudate, anterior putamen and posterior putamen of patients with PD. Correlation was evaluated for 16 patients who underwent the two examinations (scintigraphy and PET) within 6 months. In all four graphs, no significant correlations are observed between the early images (*open circles*) and delayed images (*plus signs*)

previous meta-analysis of studies with a total of 246 PD cases [36], in both early and delayed images our study showed high specificity for the overall cases and high sensitivity for the advanced cases. However, early cases tended to have relatively lower sensitivity in both images, although the sample size and methodology greatly differed among the studies. Thus, our results suggested that even in the case of sustained cardiac ^{123}I-MIBG uptake, the possibility of PD should not be denied and follow-up clinical examinations, including ^{123}I-MIBG scintigraphy, should be conducted, especially in early and mild PD cases.

No definite correlation was found either between cardiac ^{123}I-MIBG uptake and striatal ^{11}C-CFT uptake or between cardiac ^{123}I-MIBG uptake and subregional ^{11}C-CFT uptake in the PD group. Two groups have reported the association between the functional impairment of the nigrostriatal dopaminergic system and that of the cardiac sympathetic system [8, 37]. Spiegel et al. (n=18) found a correlation between the two indices, i.e. ^{123}I-MIBG and ^{11}C-CFT uptake, while Raffel et al. (n=9) found no correlation between them. This discrepancy may be explained as follows. The functional impairment of both the nigrostriatal dopaminergic and cardiac sympathetic systems increases with disease progression, as described earlier; hence, a correlation was observed in some studies. On the other hand, there is no report that suggests a direct cause-effect relationship between the functional impairment of the nigrostriatal dopaminergic system and that of the cardiac sympathetic system. Thus, a statistically significant correlation between the functional impairments of the two systems may depend on the sample size and methodology. However, the functional impairments of the two systems would, in fact, occur and progress independently. Sometimes, impairment of the cardiac sympathetic function may precede that of the nigrostriatal dopaminergic function, while at other times, the latter may precede the former.

This is the first report wherein PD and NPD patterns in dopamine PET findings were defined on the basis of the results which have been confirmed as follows. In presynaptic DAT images, three characteristic changes are observed [14–16, 22]. First, the reduction in the ^{11}C-CFT uptake in the striatum begins from the posterior putamen, representing the initial locus of PD [38]. Second, the uptake ratio of the posterior putamen to the caudate is less than 1. Third, one putamen is usually more affected than the other, reflecting asymmetric degeneration. In fact, Fig. 4 shows that the ^{11}C-CFT uptake in the posterior putamen markedly decreased in the early stage of PD, while that in the caudate was relatively constant in the early stage. In postsynaptic D_2R images, putaminal uptake is normal or mildly upregulated in untreated PD, presumably as a compensatory response to decrease in presynaptic dopamine [17–19]. On the other hand, in treated or longstanding PD, the uptake restores to the normal level in the putamen and most often decreases in the caudate; this is presumably as a result of long-term downregulation due to chronic dopaminergic therapy or structural adaptation of the postsynaptic dopaminergic system to the progressive degeneration of nigrostriatal neurons [17, 19, 21]. In fact, in vitro studies have reported that the densities of striatal D_2Rs are maintained even in the advanced stage [39, 40].

On the basis of the earlier mentioned characteristic changes, especially in the posterior putamen, we defined the PD and NPD patterns such that false-negative cases should be as few as possible, because the aim was to reinforce the published clinical criteria. For defining the PD pattern, we considered that ^{11}C-CFT uptake in the posterior putamen of the patients should be less than that in the caudate of the patients and less than 50% of the mean uptake in normal controls. This percentage (i.e. 50%) was selected (1) on the basis of previous PET reports and considered suitable to distinguish normal from affected individuals [14–16, 22] and (2) on the basis of previous reports of in vitro studies, stating that parkinsonian symptoms appear when 80% of the striatal dopamine is lost or 50% of the nigral cells degenerate [38, 41]. Asymmetric uptake was not defined because of the difficulty in determining the intraindividual differences in